

TECHNICAL REPORT

ISIS-06-710

Analytical solution for radio-interferometric localization of mobile sensors

Branislav Kusý and János Sallai

Institute for Software Integrated Systems,
Vanderbilt University, Nashville, TN, USA

Abstract. Radio-interferometric ranging [2] offers an alternative to terrestrial GPS for localization and tracking in wireless sensor networks. Because of the excessive computational costs of ranging and localization, a PC class server is required to compute the locations using the measurement data collected by the low-power resource constrained sensor nodes. This report proposes an analytical location solver that would fit in a low-power self-contained hardware implementation, analogous to a GPS receiver. A technique to measure the speed and direction of the moving node using the Doppler effect is also proposed.

1 Introduction

Radio-interferometric ranging [2] [1] is a novel technique that allows for fine-grained localization and tracking of mobile wireless sensor nodes. This technique relies on two nodes transmitting pure sine waves at close frequencies, thus generating an interference field. Receivers measure the phase of the low frequency beat signal. The offset of phases measured at two receivers carry location related information.

$$d_{ABCD} \bmod \lambda = \varphi_{CD} \frac{\lambda}{2\pi}, \quad (1)$$

where A and B are the transmitter nodes, λ is the wavelength corresponding to the average of the two carrier frequencies, φ_{CD} is the relative phase difference measured by nodes C and D , and d_{ABCD} is the interferometric range (denoted as q-range). The q-range is defined by the equation

$$d_{ABCD} = d_{AD} + d_{BC} - d_{AC} - d_{BD} \quad (2)$$

where d_{XY} is the Euclidean distance between X and Y .

Notice that Eq. (1) has an infinite number of solutions. To overcome this problem, q-ranges are measured at different frequencies: it has been reported

that measuring at eleven different channels yield good results in an environment with moderate multipath.

When the locations of three of the four nodes contributing to a q-range measurement are known, a quantity relating the positions of three nodes can be derived. Without loss of generality, let us assume that the position of node A is unknown, while the positions of the remaining four nodes are given. Let us rearrange Eq. (2) such that the known quantities are on the left hand side:

$$d_{ABCD} - d_{BC} + d_{BD} = d_{AD} - d_{AC}$$

Let us denote the left hand side with the term t -range. The t -range d_{ACD} relates the location of three nodes, constraining the location of node A on a hyperbola (in two dimensions) with foci C and D .

$$d_{ACD} = d_{AD} - d_{AC} \quad (3)$$

The t -range d_{ACD} can be computed from the q-range measurement and the known anchor locations. Given multiple t -ranges, the position of the unknown node can be computed as the intersection of the corresponding hyperbolae.

In the general case, however, calculating the target location this way have drawbacks: 1) two conic sections can have as many as 4 points of intersection, and 2) analytical solution is not feasible. To overcome these problems, in Section 3 we propose to solve a special case analytically, where the two hyperbolae share a focus. This approach yields unambiguous results, allows for analytical sensitivity analysis and poses minimal limitations on the anchor placement.

In Section 2.2, we present a technique that uses the Doppler effect to compute a speed-related quantity, denoted as the q-speed using the frequencies measured by the receiver nodes at different frequencies. When the calculated locations are available, q-speeds can be converted to velocity vectors (actual speed with direction).

2 Intersection of hyperbolae

Theorem 1. *Consider Figure 1: hyperbola h_{AB} is defined by its foci A, B and the distance R_{AB} such that for any point $X \in h_{AB}$, $|AX| - |BX| = R_{AB}$. Similarly, h_{AC} is defined by the foci A, C , and the distance R_{AC} . Given the coordinates of A, B, C and the distances R_{AB}, R_{AC} , find the intersection points of h_{AB}, h_{AC} .*

Proof. The following equations hold for the hyperbolae:

$$\begin{aligned} \sqrt{x^2 + y^2} - \sqrt{(x - b)^2 + y^2} &= R_{AB} \\ \sqrt{x^2 + y^2} - \sqrt{(x - c_x)^2 + (y - c_y)^2} &= R_{AC} \end{aligned}$$

moving $\sqrt{x^2 + y^2}$ to the other side and squaring we get:

$$\begin{aligned} x^2 + y^2 - 2\sqrt{x^2 + y^2}R_{AB} + R_{AB}^2 &= (x - b)^2 + y^2 \\ x^2 + y^2 - 2\sqrt{x^2 + y^2}R_{AC} + R_{AC}^2 &= (x - c_x)^2 + (y - c_y)^2 \end{aligned}$$

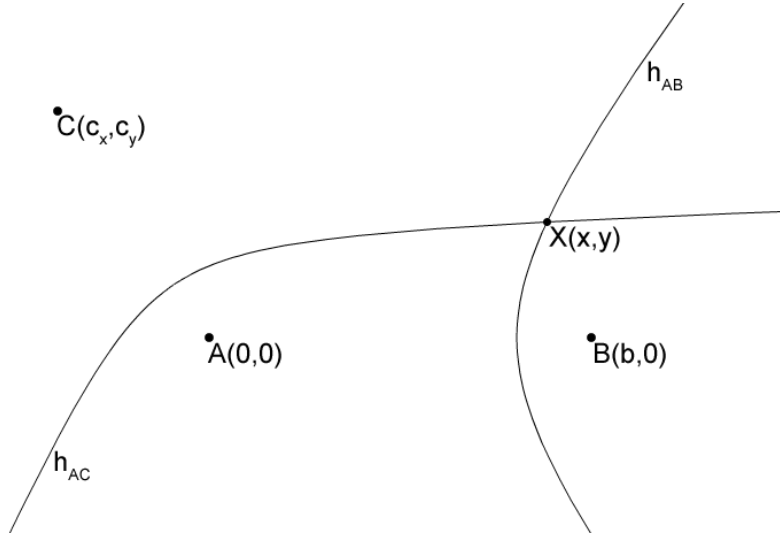


Fig. 1. Two hyperbolae given by their foci A, B and A, C .

We further adopt the following notation the foci, semimajor and semiminor axis lengths of h_{AB}, h_{AC} :

$$\begin{aligned} A_{AB} &= R_{AB}/2, & A_{AC} &= R_{AC}/2, \\ C_{AB} &= b/2, & C_{AC} &= c/2 = \sqrt{c_x^2 + c_y^2}/2, \\ B_{AB} &= \sqrt{b^2 - R_{AB}^2}/2, & B_{AC} &= \sqrt{c^2 - R_{AC}^2}/2 \end{aligned}$$

We simplify the equations:

$$\begin{aligned} \sqrt{x^2 + y^2}R_{AB} &= bx - 2B_{AB}^2 & (4) \\ \sqrt{x^2 + y^2}R_{AC} &= c_x x + c_y y - 2B_{AC}^2 \end{aligned}$$

Next we equate the two equations and substitute one into the other:

$$(bR_{AC} - c_x R_{AB})x = 2B_{AB}^2 R_{AC} + c_y R_{AB} y - 2B_{AC}^2 R_{AB} \quad (5)$$

We substitute D, E as follows and rewrite (5)

$$\begin{aligned} D &= c_y R_{AB} / (bR_{AC} - c_x R_{AB}) \\ E &= 2(B_{AB}^2 R_{AC} - B_{AC}^2 R_{AB}) / (bR_{AC} - c_x R_{AB}) \\ x &= Dy + E \end{aligned} \quad (6)$$

We substitute (6) into (4):

$$\sqrt{(Dy + E)^2 + y^2} = \frac{b}{R_{AB}}(Dy + E) - 2\frac{B_{AB}^2}{R_{AB}} \quad (7)$$

We further define:

$$F = \frac{bE - 2B_{AB}^2}{R_{AB}}$$

and rewrite (7) into:

$$D^2y^2 + 2DEy + E^2 + y^2 = \frac{b^2D^2}{R_{AB}^2}y^2 + 2\frac{bDF}{R_{AB}}y + F^2$$

which is a quadratic equation in y :

$$(1 + D^2 - \frac{b^2D^2}{R_{AB}^2})y^2 + (2DE - 2\frac{bDF}{R_{AB}})y + E^2 - F^2 = 0 \quad (8)$$

The discriminant of (8) is denoted with Disc_y :

$$\begin{aligned} \text{Disc}_y &= (2DE - 2\frac{bDF}{R_{AB}})^2 - 4(1 + D^2 - \frac{b^2D^2}{R_{AB}^2})(E^2 - F^2) \\ &= 4(F^2 - E^2) + 4D^2(\frac{F^2 + b^2E^2}{R_{AB}^2} - \frac{2bEF}{R_{AB}}) \end{aligned}$$

Solutions of (8) along with (6) give us intersection points of the two hyperbolae:

$$\begin{aligned} y_1 &= \frac{-(2DE - 2\frac{bDF}{R_{AB}}) + \sqrt{\text{Disc}_y}}{2(1 + D^2 - \frac{b^2D^2}{R_{AB}^2})} \\ y_2 &= \frac{-(2DE - 2\frac{bDF}{R_{AB}}) - \sqrt{\text{Disc}_y}}{2(1 + D^2 - \frac{b^2D^2}{R_{AB}^2})} \end{aligned}$$

2.1 Degenerate cases

The quadratic formula assumes that the all coefficient of Eq. 8 be finite, and that the coefficient of y^2 be non-zero. Otherwise the formula is not applicable, and alternate ways of finding the solution need be used.

a. The coefficient of the quadratic term is zero. As the coefficient of the quadratic term approaches zero, one of the solutions go to (minus) infinity. The parabola becomes a line, hence the quadratic equation will behave like a linear equation.

Testing for this degenerate case is carried out by checking if the coefficient of the quadratic term is zero, i.e. if the following equality holds:

$$1 + D^2 - \frac{b^2D^2}{R_{AB}^2} = 0$$

It can be shown that if the two hyperbolae have parallel asymptotes, the above equality will hold.

There are two options to find the solution for this degenerate case:

– Solve Eq. 8 as a linear equation.

$$(2DE - 2\frac{bDF}{R_{AB}})y + E^2 - F^2 = 0 \quad (9)$$

– Add a small number ϵ to R_{AB} (or R_{AC}), such that the coefficient of the quadratic term becomes non-zero, and solve Eq. 8.

b. Non-finite coefficients. As the term $b_x R_{AC} - c_x R_{AB}$ can be found in denominators in all three of the coefficients, the coefficients go to infinity if this term goes to zero.

Multiplying the coefficients with $(b_x R_{AC} - c_x R_{AB})^2$ will cancel out the denominators and thus solves the problem. The coefficients can be further simplified by dividing them by $(R_{AB}^2 R_{AC}^2)$. The new coefficients, after simplifications, are the following:

$$\begin{aligned} a &= 4R_{AB}^2(c_x^2 + c_y^2) + 4b_x^2(R_{AC}^2 - c_y^2) - 8b_x c_x R_{AB} R_{AC} \\ b &= 4c_y(R_{AB}^2 - b_x^2)(b_x c_x - R_{AB} R_{AC} - c_x^2 - c_y^2 + R_{AC}^2) \\ c &= (R_{AB}^2 - b_x^2)((b_x c_x - R_{AB} R_{AC} - c_x^2 - c_y^2 + R_{AC}^2)^2 \\ &\quad - (c_x R_{AB} - b_x R_{AC})^2) \end{aligned}$$

c. The discriminant is zero. The discriminant corresponding to the above coefficients is

$$\begin{aligned} d &= 16(c_x^2 + c_y^2 - R_{AC}^2)(b_x^2 - R_{AB}^2)((b_x - c_x)^2 + c_y^2 \\ &\quad - (R_{AB} - r_{AC})^2) + (b_x R_{AC} - c_x R_{AB})^2 \end{aligned}$$

The first, second and third terms of the product are never zero unless the position of the target coincides with anchor A or C, A or B, and B or C, respectively. The last term can be zero without any such coincidences. As the last term approaches zero, the two solutions, the correct and the false one, get closer to each other and are more difficult to distinguish between them just by substituting back to the original hyperbola equations.

2.2 Sensitivity analysis

The coordinates of the target are computed from the measured distance differences R_{AB} and R_{AC} . Formally, R_{AB} and R_{AC} are parameters of an algebraic expression. Here we investigate how sensitive the calculated coordinates are to the input parameters.

Let us rewrite Eq. 8 the following way.

$$a(R_{AB}, R_{AC})y^2 + b(R_{AB}, R_{AC})y + c(R_{AB}, R_{AC}) = 0$$

The discriminant of the above equation, as a function of R_{AB} and R_{AC} has the following form:

$$d(R_{AB}, R_{AC}) = b^2(R_{AB}, R_{AC}) - 4a(R_{AB}, R_{AC})c(R_{AB}, R_{AC})$$

Substituting the coefficients into the quadratic formula, we get the solution for the y coordinate of the target as a function of the parameters:

$$y_{1,2}(R_{AB}, R_{AC}) = \frac{-b(R_{AB}, R_{AC}) \pm \sqrt{d(R_{AB}, R_{AC})}}{2a(R_{AB}, R_{AC})}$$

To analyze the sensitivity of the output to errors of the inputs, we take the partial derivatives of $y_{1,2}(R_{AB}, R_{AC})$ with respect to both parameters.

$$\begin{aligned} \frac{\partial y_{1,2}}{\partial r_{AB}} &= \frac{-\frac{\partial b}{\partial r_{AB}} \pm \frac{\partial d}{\partial r_{AB}} \frac{1}{2\sqrt{d}}}{2a} - \frac{\frac{\partial a}{\partial r_{AB}} (-b \pm \sqrt{d})}{2a} \\ \frac{\partial y_{1,2}}{\partial r_{AC}} &= \frac{-\frac{\partial b}{\partial r_{AC}} \pm \frac{\partial d}{\partial r_{AC}} \frac{1}{2\sqrt{d}}}{2a} - \frac{\frac{\partial a}{\partial r_{AC}} (-b \pm \sqrt{d})}{2a} \end{aligned}$$

Since $a(R_{AB}, R_{AC})$, $b(R_{AB}, R_{AC})$, $c(R_{AB}, R_{AC})$ and $d(R_{AB}, R_{AC})$ are all polynomials, the partial derivatives exist and are finite except where $a(R_{AB}, R_{AC})$ or $d(R_{AB}, R_{AC})$ is zero.

For any target position, only one of the roots gives a correct result. It can be shown that the correct solution is

$$y = \begin{cases} y_1, & R_{AC} \leq R_{AB} \frac{c_x}{b_x} \\ y_2, & R_{AC} > R_{AB} \frac{c_x}{b_x} \end{cases}$$

(If $R_{AC} = R_{AB} \frac{c_x}{b_x}$ the discriminant is zero, hence y_1 and y_2 are equal.) Similarly, for the partial derivatives,

$$\frac{\partial y}{\partial R_{AB}} = \begin{cases} \frac{\partial y_1}{\partial R_{AB}}, & R_{AC} \leq R_{AB} \frac{c_x}{b_x} \\ \frac{\partial y_2}{\partial R_{AB}}, & R_{AC} > R_{AB} \frac{c_x}{b_x} \end{cases}$$

and,

$$\frac{\partial y}{\partial R_{AC}} = \begin{cases} \frac{\partial y_1}{\partial R_{AC}}, & R_{AC} \leq R_{AB} \frac{c_x}{b_x} \\ \frac{\partial y_2}{\partial R_{AC}}, & R_{AC} > R_{AB} \frac{c_x}{b_x} \end{cases}$$

The partial derivatives $\frac{\partial y}{\partial R_{AB}}$ and $\frac{\partial y}{\partial R_{AC}}$ evaluated at R_{AB} and R_{AC} corresponding to a given anchor placement and a reference point yields the sensitivity of the calculated coordinates to the error in the inputs if the target is at the reference point.

The following plot of the partial derivatives illustrate the sensitivity of the computation for target positions $([-200..200], [-200..200])$ to parameters R_{AB} and R_{AC} , respectively. The anchor nodes are A(0,0), B(100,0), C(60,80).

As we can see in the above example, the parallelogram defined by A, B, C and the reflected image of A to the BC line is a region where both partial derivatives are between -1 and 2. We have empirically verified that this parallelogram is a safe region if the angle of BA and AC is obtuse. That is, if the target is within this parallelogram, the amplification of ranging errors is less than twofold.

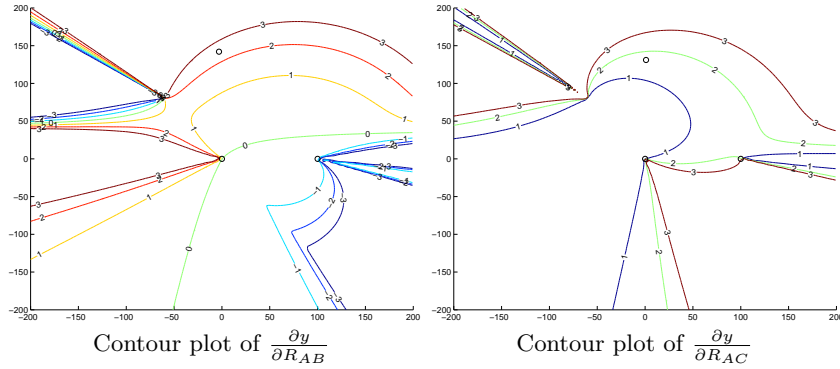


Fig. 2. Sensitivity of the computation with respect to R_{AB} and R_{AC} . Contour curves above 3 and below -3 are not plotted. The anchor nodes are A(0,0), B(100,0), C(60,80).

3 Moving Nodes

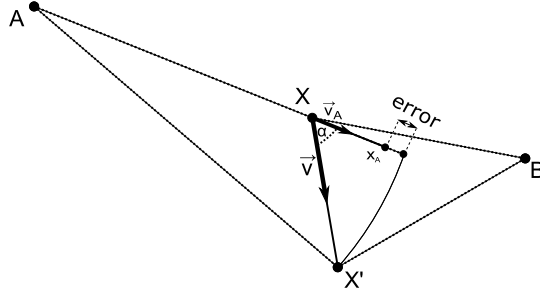


Fig. 3. Doppler compensation

Let A and X be the locations of an anchor and a target node. Let α be the angle between \overrightarrow{AX} and the velocity vector \vec{v} and \vec{v}_a be the component vector of \vec{v} parallel with \overrightarrow{AX} . Let $v_a = |\vec{v}_a|$, if \vec{v}_a and \overrightarrow{AX} have the same direction and $v_a = -|\vec{v}_a|$ otherwise. If t is the measurement time, the target covers the distance $|XX'| = |\vec{v}|t$ along the direction of \vec{v} , and the distance $x_A = v_a t$ along the direction of \vec{v}_a .

Theorem 2. Let us define a function

$$\varepsilon(\alpha) = d_{AX'} - d_{AX} - x_a.$$

The extremal points of $\varepsilon(\alpha)$ are at a.) $\alpha = 0$, and b.) $\alpha = \arccos -\frac{d_{XX'}}{2d_{AX}}$.

Proof. For the case shown in Fig. 3, we can use the definition of cosine and the law of cosines, and calculate

$$\begin{aligned} |\vec{v}_a|t &= d_{XX'} \cos \alpha, \\ d_{AX'} &= \sqrt{d_{AX}^2 + d_{XX'}^2 + 2d_{AX}d_{XX'} \cos \alpha}. \end{aligned}$$

Since we are interested in the extremes of $\varepsilon(\alpha)$, let us differentiate both $|\vec{v}_a|t$ and $d_{AX'}$:

$$\begin{aligned} \frac{d(|\vec{v}_a|t)}{d(\alpha)} &= -d_{XX'} \sin \alpha, \\ \frac{d(d_{AX'})}{d(\alpha)} &= \frac{d_{AX}d_{XX'} \sin \alpha}{\sqrt{d_{AX}^2 + d_{XX'}^2 + 2d_{AX}d_{XX'} \cos \alpha}} \end{aligned}$$

Let us consider 2 cases:

$|\alpha| \leq \frac{\pi}{2}$: we know that $x_a = |\vec{v}_a|t$, so we need to find the extremes of $\varepsilon(\alpha) = d_{AX'} - d_{AX} - |\vec{v}_a|t$. We do this by differentiating $\frac{d(\varepsilon(\alpha))}{d(\alpha)}$:

$$\begin{aligned} \frac{d(\varepsilon(\alpha))}{d(\alpha)} &= \frac{d(d_{AX'})}{d(\alpha)} - \frac{d(d_{AX})}{d(\alpha)} - \frac{d(|\vec{v}_a|t)}{d(\alpha)} \\ &= \frac{-d_{AX}d_{XX'} \sin \alpha}{\sqrt{d_{AX}^2 + d_{XX'}^2 + 2d_{AX}d_{XX'} \cos \alpha}} + d_{XX'} \sin \alpha \end{aligned}$$

Now we let $\frac{d(\varepsilon(\alpha))}{d(\alpha)} = 0$. It is easy to see that either $\sin \alpha = 0$, or:

$$\frac{d_{AX}}{\sqrt{d_{AX}^2 + d_{XX'}^2 + 2d_{AX}d_{XX'} \cos \alpha}} = 1$$

from where $\cos \alpha = -\frac{d_{XX'}}{2d_{AX}}$.

Since $\cos \alpha$ is negative only for $|\alpha| > \frac{\pi}{2}$, the extremal point is attained at $\pm \frac{\pi}{2}$.

To summarize, $\varepsilon(\alpha)$ attains its minimum at $\alpha = 0$ and its maximum at $\pm \frac{\pi}{2}$ in this case.

$|\alpha| \geq \frac{\pi}{2}$: similarly, $x_a = -|\vec{v}_a|t$, so we find the extremes of $\varepsilon(\alpha) = d_{AX'} - d_{AX} + |\vec{v}_a|t$:

$$\frac{d(\varepsilon(\alpha))}{d(\alpha)} = \frac{-d_{AX}d_{XX'} \sin \alpha}{\sqrt{d_{AX}^2 + d_{XX'}^2 - 2d_{AX}d_{XX'} \cos \alpha}} + d_{XX'} \sin \alpha$$

Performing the same steps as in the previous case, we conclude that the minimum is attained at $\alpha = \pi$ and the maximum is attained at $\cos \alpha = -\frac{d_{XX'}}{2d_{AX}}$. $\varepsilon(\alpha)$ has a local minimum at $\alpha = \frac{\pi}{2}$ but this is definitely larger than 0 attained at $\alpha = 0$.

Since $\varepsilon(\alpha)$ is larger for $\alpha = \arccos -\frac{d_{XX'}}{2d_{AX}}$ than at $\alpha = \frac{\pi}{2}$ (proof of the second case), we can conclude that $\varepsilon(\alpha)$ attains the global minimum at $\alpha = 0$ and the global maximum at $\arccos -\frac{d_{XX'}}{2d_{AX}}$.

4 Conclusion

In this report, we presented an analytical solver that computes the intersection of two hyperbolae in a special case when they share a common focus. We intend to use this solver to compute mobile node locations in radio-interferometric tracking, however, it is applicable to a variety of multilateration problems, e.g. to solve TDOA equations analytically. We also introduced a method to calculate the velocity vector of the tracked target using radio-interferometric frequency measurement and the previously calculated node location. This approach, leveraging the Doppler effect, when coupled with the analytical location solver, can be used to compute the location, speed and direction of the tracked node using only two measurement rounds.

References

1. B. Kusý, G. Balogh, P. Völgyesi, J. Sallai, A. Nádas, A. Lédeczi, M. Maróti, and L. Meertens. Node-density independent localization. *Information Processing in Sensor Networks (IPSN 06) SPOTS Track*, Apr. 2006.
2. M. Maróti, B. Kusý, G. Balogh, P. Völgyesi, A. Nádas, K. Molnár, S. Dóra, and A. Lédeczi. Radio interferometric geolocation. *in Proc. ACM 3rd Conference on Embedded Networked Sensor Systems (SenSys)*, Nov. 2005.